

Ductility and Ultimate Capacity of Concrete-Filled Lattice Rectangular Steel Tube Columns

Chengquan Wang¹, Yun Zou^{1,*}, Tianqi Li¹, Jie Ding¹, Xiaoping Feng¹ and Tiange Lei¹

Abstract: A kind of concrete-filled lattice rectangular steel tube (CFLRST) column was put forward. The numerical simulation was modeled to analyze the mechanical characteristic of CFLRST column. By comparing the load-deformation curves from the test results, the rationality and reliability of the finite element model has been confirmed, moreover, the change of the section stiffness and stress in the forcing process and the ultimate bearing capacity of the column were analyzed. Based on the model, the comparison of ultimate bearing capacity and ductility between CFLRST column and reinforced concrete (RC) column were also analyzed. The results of the finite element analysis show that the loading process of CFLRST column consists of elastic stage, yield stage and failure stage. The failure modes are mainly strength failure and failure of elasto-plastic instability. CFLRST column has higher bearing capacities in comparison with reinforced concrete columns with the same steel ratio. In addition, the stiffness degeneration of CFLRST column is slower than RC column and CFLRST column has good ductility.

Keywords: Steel-concrete composite structure, concrete-filled lattice rectangular steel tube column, nonlinear finite element, ultimate strength, ductility.

1 Introduction

Due to the great advantages, such as high strength, favorable ductility and good seismic behavior, concrete-filled steel tubular columns have been widely used in the construction of high-rise buildings [Liew and Xiong (2012)].

Generally speaking, if the cross-sectional areas are the same a square CFDT column would have higher flexural stiffness than the circular column. Meanwhile, a square column is easier to connect with the beam. Therefore, this paper will focus on the study of square columns.

In this paper, A kind of concrete-filled lattice rectangular steel tube (CFLRST) column was put forward. The numerical simulation was modeled to analyze the mechanical characteristic of CFLRST column by using finite element software ABAQUS.

¹ Jiangnan University, No. 1800, Wuxi, 214000, China.

* Corresponding Author: Yun Zou. Email: zouyun_22@126.com.

2 Finite element modeling

A new type of rectangular concrete-filled steel tube column was presented in this paper, as shown in Fig. 1 and Fig. 2. Through the welding of angle steel and rectangle steel plate to form lattice rectangular steel tube, the stirrups were set around the steel tube, and the reinforcing rebars were set up at the same time, at last the core concrete and outer concrete were poured.

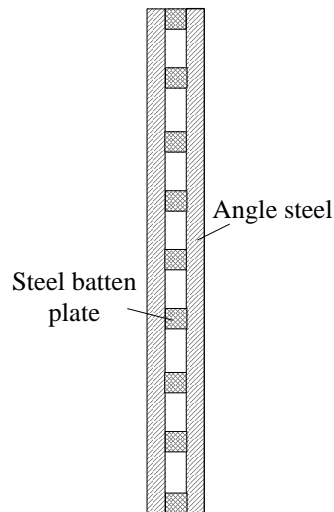


Figure 1: Elevation design of lattice rectangular steel tube

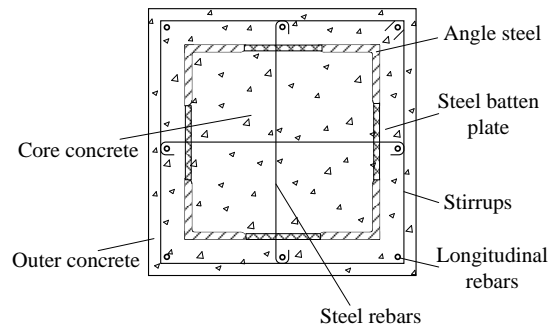


Figure 2: Cross-sectional diagram

The general-purpose finite element program ABAQUS was used in this paper to build a FE model for CFLRST columns and RC columns. The 8-node brick elements with three translation degrees of freedom attach node (C3D8R) were used to model the steel tube and concrete; Truss element (T3D2) is the linear component can only withstand tensile and compressive loads in space, which was used to simulate the stirrups and longitudinal rebars. The FE model were shown in Fig. 3 and Fig. 4. The size of the model grid was 0.01 M, and the sweep grid division technique was used to divide the model, and the FE model was set up 62958 units.

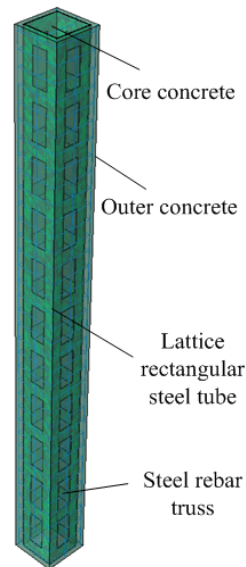


Figure 3: FE model of CFRST column

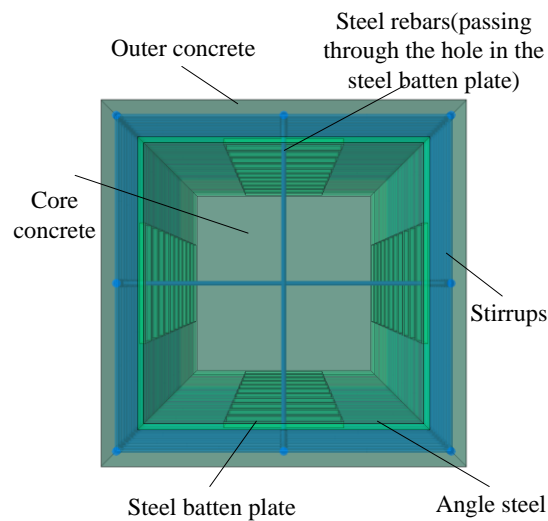


Figure 4: Cross sectional of CFRST column FE model

2.1 Material properties

The damage-plasticity model was used in the FE model for simulate the concrete [Wang, Tao and Yu (2017)]. The value of dilation Angle (ψ) was 35° , which was determined by Eq. (1), the flow potential eccentricity was taken as the default value of 0.1; Calculated by Eq. (2) the ratio of the compressive strength under biaxial loading to uniaxial compressive strength (f_{b0} / f_{c0}) was 1.16; Invariable stress ratio (K_c) was calculated by Eq.

(3), which was 0.667, the viscosity parameter was 0.0005 [Romero, Ibañez, Espinos et al. (2016)].

$$\psi = \begin{cases} 56.3(1-\xi)^{\frac{7.4}{4.64+\xi}} & \text{for } \xi \leq 0.5 \\ 6.672e^{\frac{7.4}{4.64+\xi}} & \text{for } \xi > 0.5 \end{cases} \quad (1)$$

$$K_c = \frac{5.5}{5 + 2(f'_c)^{0.075}} \quad (2)$$

$$f_{bo} / f'_c = 1.5(f'_c)^{-0.075} \quad (3)$$

The relation model Saenz was used to simulate the concrete uni-axial compression stress and strain relations, which is shown in Fig. 5.

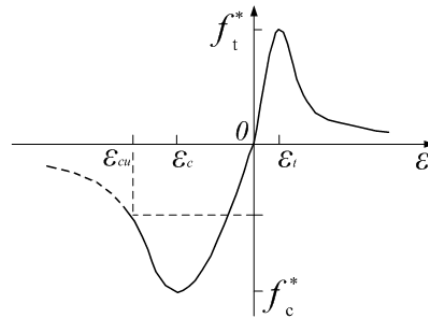


Figure 5: Compressive stress-strain relation of concrete

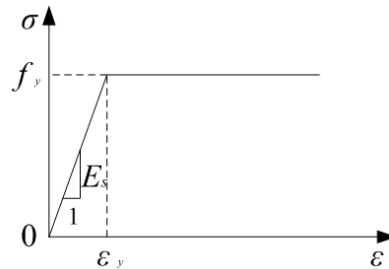


Figure 6: Steel constitutive relation

The constitutive relationship of steel tube, steel rebar is perfectly plastic model, which is shown in Fig. 6.

2.2 The connection between steel and concrete

Surface-to-surface contact is usually used for the interaction simulation of the steel tube and concrete. A contact surface pair comprised of the inner surface of the steel tube and the outer surface of concrete core can be defined. “Hard contact” in the normal direction can be specified for the interface, which allows the separation of the interface in tension and no penetration of that in compression. The tangent contact can be simulated by the

Coulomb friction model, in which the coefficient of friction between the steel tube and concrete was taken as 0.4.

2.3 Boundary condition and solving method

In avoidance of the local buckling of the steel tube initiating at the ends [Uy (2001); Young (2006)], the end plates and stiffeners were set in the FE model. All three translational degrees of freedom can be restrained for the ends of the column except the vertical displacement at the loaded end.

The finite element model was loaded by the displacement control, and the "Static General" algorithm was adopted in the analysis step, and the geometric nonlinear effect was considered.

3 Analysis of finite element results

3.1 Strain and stress analysis

Fig. 7 shows the results of longitudinal strain of components in CFLRST column. From the diagram, it can be seen that lattice rectangular steel tube, rebar and core concrete generate the maximum deformation in the middle of the part when CFLRST column failed. Moreover, the central deformation of lattice rectangular steel tube, rebar and core concrete are 0.03523, 0.02879 and 0.03287, respectively, which demonstrates all the parts have good synergistic effect.

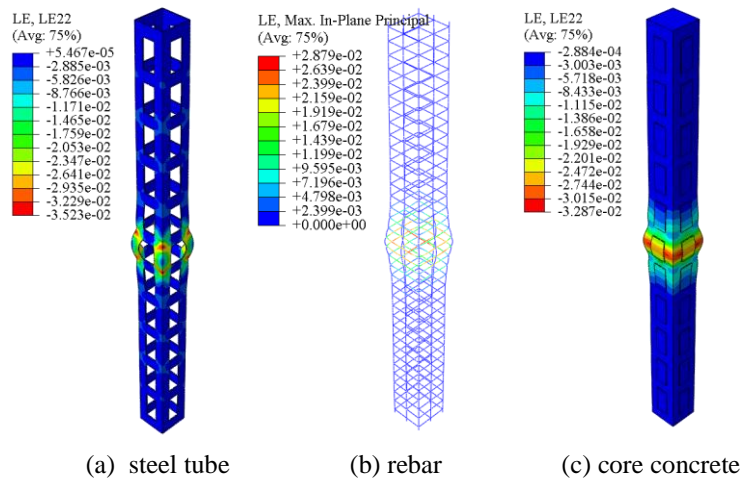


Figure 7: Longitudinal strain of components in CFLRST column

Longitudinal stress of all the parts in CFLRST column was obtained as shown in Fig. 8. The diagram shows that rebar and lattice rectangular steel tube reached yield strength when CFLRST column failed. In addition, Central concrete connected with angel steel also reached ultimate compressive strength of concrete, which demonstrates that angel steel has a strong blinding effect on core concrete.

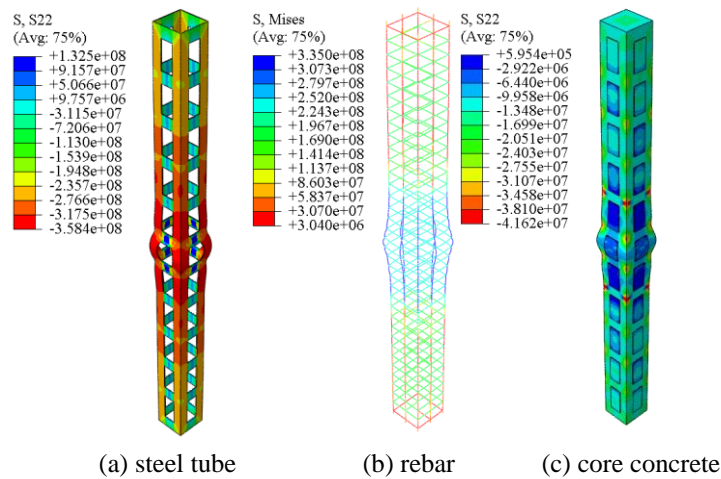


Figure 8: Longitudinal stress of components in CFLRST column

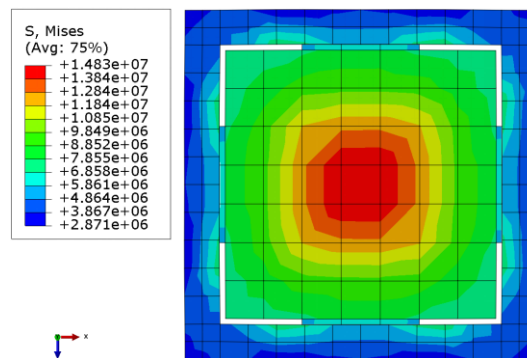


Figure 9: Concrete stress nephogram of CFLRST column section

Fig. 9 shows that the stress distribution in the confinement area of the core concrete in CFLRST column is round, and the distribution pattern is similar to that of the circular concrete-filled steel tube column. Thus it can be seen that the core concrete constraint effect of the CFLRST column is better than the traditional rectangular concrete filled steel tube column.

3.2 Failure state analysis

The failure modes/deformation of CFLRST column have been simulated, which was shown in Fig. 10.

The figure shows that CFLRST column failed by local outward buckling of the outer lattice rectangular steel tube, and the buckling of the outer steel tube did not occur until the outer concrete was crushed and angle steel buckled.

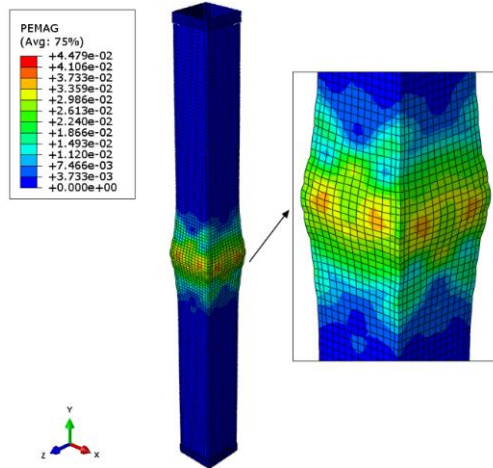


Figure 10: The failure modes of CFLRST column

3.3 Comparison of ultimate bearing capacity

After the analysis, the vertical load - axial displacement curve of the CFLRST column was shown in Fig. 11.

The figure shown that CFLRST column can be divided into four stages from loading to failure: elastic stage and nonlinear rising stage from concrete cracking to steel tube yielded, the strengthening stage of yielded steel tube and the decline stage after the ultimate bearing capacity.

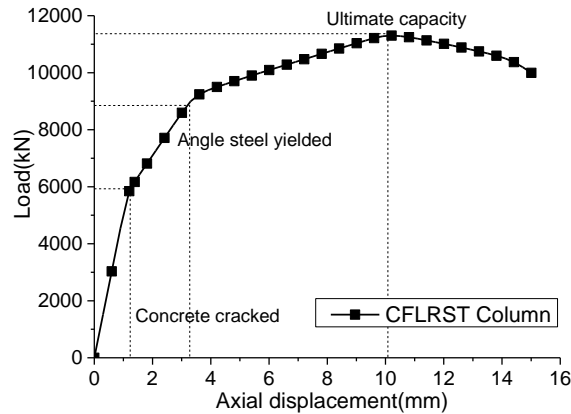


Figure 11: Axial displacement-load curves of CFLRST column and RC column

For assessing the bearing capacity of CFLRST column directly, a finite element model of reinforced concrete (RC) column with same section steel ratio was modeled. The load - axial displacement curve of the RC column was shown in Fig. 12. The comparison of bearing capacity between CFLRST column and RC column was listed in Tab. 1.

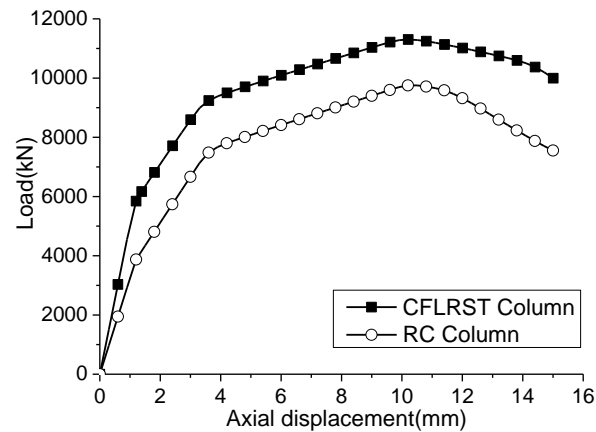


Figure 12: Axial displacement-load curves of CFLRST column and RC column

Table 1: Comparison of bearing capacity between CFLRST column and RC column

Column specimen	Cracking load P_c /kN	Yield load P_y /kN	Ultimate load P_u /kN
CFLRST column	5842.58	8996.06	11302.1
RC column	3872.61	7129.96	9753.41

From Tab. 1, it can be seen that the bearing capacity of CFLRST column was higher than that of RC column. Due to the constraint of outer lattice rectangular steel tube, the cracking load of CFLRST column was 1.51 times of the RC column, the yield load of CFLRST column was 1.26 times of the RC column, and the ultimate load was 1.16 times of the RC column.

3.4 Stiffness degradation analysis of CFLRST column

In this paper, at first the calculation method from the paper Ho et al. [Ho and Dong (2014)] is used to analyze the stiffness of column section K , which determined as follows:

$$K = \frac{|P_i|}{|\Delta_i|} \quad (4)$$

Where P_i is the i -level load, Δ_i is the mid-span deflection corresponding the i -level load.

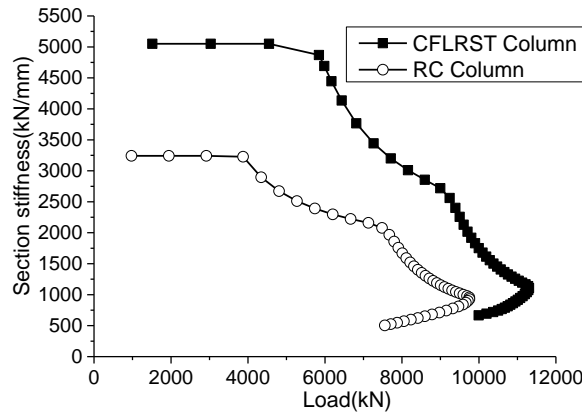


Figure 13: Section stiffness-load curves of CFLRST column and RC column

Fig. 13 shows that section stiffness-load curves of CFLRST column and RC column, respectively. In the diagram, the stiffness of CFLRST column lower significantly when the load reaches 5842.58 kN, which is higher than cracking load of RC column with 3872.61 kN. Therefore, it can be found that the stiffness degradation of CFLRST column was postponed in comparison with RC column. When load reaches 8996.06 kN, the stiffness of CFLRST column reduced further with buckling of angel steel. From the picture, it can be seen that CFLRST column generate the second stiffness degradation more lately.

3.5 Analysis of ductility

According to the definition method of the ductility of rectangular concrete-filled steel tube column in paper Wang et al. [Wang, Tao, Han et al. (2017)], the ductility index of the composite column was defined as:

$$DI = \Delta_{85\%} / \Delta_u \tag{5}$$

Where, Δ_u is the axial displacement corresponding to the ultimate load; $\Delta_{85\%}$ is the axial displacement corresponding to the load go down to 85% of the ultimate load. It was calculated that the ductility coefficient of each column was shown in Tab. 2, where a higher DI indicates a slower attenuation of load after the peak load.

In comparison with RC column, the DI of CFLRST column was improved from 1.286 to 1.529, which show that CFLRST column have a good ductility.

Table 2: Comparison of ductility between CFLRST Column and RC Column

Column specimen	DI
CFLRST Column	1.529
RC Column	1.286

4 Conclusion

1. CFLRST column has high stiffness and bearing capacities, and its ultimate bearing capacity is 1.16 times as high as that of reinforced concrete columns with the same steel ratio.
2. CFLRST column can be divided into four stages from loading to failure. The load axial displacement curve is "four folds line". The yield of lattice steel tube causes the weakening and crushing of core concrete constraint, which is the sign of the ultimate bearing capacity of the column.
3. CFLRST column has good ductility, and its ductility coefficient DI is 1.19 times that of RC Column.

Acknowledgement: This work was financially supported by the Fundamental Research Funds for the Central Universities (JUSRP11819), National Natural Science Foundation of China through Grant 51378240, 2015 Jiangsu provincial building energy saving and construction industry science and technology project, 2016 Jiangsu provincial construction industry modernization base project.

References

- ABAQUS.** (2010): *Abaqus Scripting Users Manual. Version 6.12.* Rhode Island, USA.
- Aslani, F.; Uy, B.; Wang, Z.; Patel, V.** (2016): Confinement models for high strength short square and rectangular concrete-filled steel tubular columns. *Steel & Composite Structures*, vol. 22, no. 5, pp. 937-974.
- Chitawadagi, M. V.; Narasimhan, M. C.; Kulkarni, S. M.** (2010): Axial capacity of rectangular concrete-filled steel tube columns - doe approach. *Construction & Building Materials*, vol. 24, no. 4, pp. 585-595.
- Ding, X. F.; Li, Z.; Cheng, S. S.; Yu, Z. W.** (2016): Composite action of hexagonal concrete-filled steel tubular stub columns under axial loading. *Thin-Walled Structures*, vol. 107, no. 10, pp. 502-513.
- Gopinath, S.; Rajasankar, J.; Iyer, N. R.; Krishnamoorthy, T. S.; Bharatkumar, B. H. et al.** (2009): A strain-based constitutive model for concrete under tension in nonlinear finite element analysis of RC flexural members. *Structural Durability & Health Monitoring*, vol. 5, no. 4, pp. 311-335.
- Hassanein, M. F.; Patel, V. I.** (2018): Round-ended rectangular concrete-filled steel tubular short columns: FE investigation under axial compression. *Journal of Constructional Steel Research*, vol. 140, pp. 222-236.
- Ho, J. C. M.; Dong, C. X.** (2014): Improving strength, stiffness and ductility of CFDST columns by external confinement. *Thin-Walled Structures*, vol. 75, no. 75, pp. 18-29.
- Javed, M. F.; Sulong, N. H. R.; Memon, S. A.; Rehman, S. K. U.; Khan, N. B.** (2017): FE modelling of the flexural behaviour of square and rectangular steel tubes filled with normal and high strength concrete. *Thin-Walled Structures*, vol. 119, pp. 470-481.

- Javidan, F.; Heidarpour, A.; Zhao, X. L.; Minkkinen, J.** (2016): Application of high strength and ultra-high strength steel tubes in long hybrid compressive members: Experimental and numerical investigation. *Thin-Walled Structures*, vol. 102, pp. 273-285.
- Liew, J. Y. R.; Xiong, D. X.** (2012): Ultra-High strength concrete filled composite columns for multi-storey building construction. *Advances in Structural Engineering*, vol. 15, no. 9, pp. 1487-1504.
- Mashiri, F. R.; Uy, B.; Tao, Z.; Wang, Z. B.** (2014): Concrete-filled VHS-to-steel fabricated section stub columns subjected to axial compression. *Journal of Constructional Steel Research*, vol. 95, no. 4, pp. 141-161.
- Montalvão, D.; Amafabia, D. A. M.** (2017): A review of structural health monitoring techniques as applied to composite structures. *Structural Durability & Health Monitoring*, vol. 11, no. 2, pp. 91-147.
- Nassirnia, M.; Heidarpour, A.; Zhao, X. L.; Minkkinen, J.** (2015): Innovative hollow corrugated columns: A fundamental study. *Engineering Structures*, vol. 94, pp. 43-53.
- Ouyang, Y.; Kwan, A. K. H.** (2018): Use of analytical lateral-axial strain relation in FE analysis of axially loaded rectangular CFST columns. *Engineering Structures*, vol. 166, pp. 142-151.
- Patel, V. I.; Liang, Q. Q.; Hadi, M. N. S.** (2017): Nonlinear analysis of biaxially loaded rectangular concrete-filled stainless steel tubular slender beam-columns. *Engineering Structures*, vol. 140, pp. 120-133.
- Patton, M. L.; Singh, K. D.** (2017): Buckling of fixed-ended concrete-filled steel columns under axial compression. *International Journal of Steel Structures*, vol. 17, no. 3, pp. 1059-1071.
- Riccio, A.; Zarrelli, M.; Caputo, F.** (2013): Damage propagation in composite structures using an embedded global-local approach. *Structural Durability & Health Monitoring*, vol. 9, no. 1, pp. 21-41.
- Romero, M. L.; Ibañez, C.; Espinos, A.; Portolés, J. M.; Hospitaler, A.** (2016): Influence of ultra-high strength concrete on circular concrete-filled dual steel columns. *Structures*, vol. 9, pp. 13-20.
- Sevim, B.** (2017). Structural response of rectangular composite columns under vertical and lateral loads. *Steel & Composite Structures*, vol. 25, no. 3, pp. 287-298.
- Silva, A.; Jiang, Y.; Castro, J. M.; Silvestre, N.; Monteiro, R.** (2017): Monotonic and cyclic flexural behaviour of square/rectangular rubberized concrete-filled steel tubes. *Journal of Constructional Steel Research*, vol. 139, pp. 385-396.
- Uy, B.** (2001): Local and post local buckling of fabricated steel and composite cross sections. *Journal of Structural Engineering*, vol. 127, no. 6, pp. 666-677.
- Wang, C.; Shen, Y.; Yang, R.; Wen, Z.** (2017): Ductility and ultimate capacity of prestressed steel reinforced concrete beams. *Mathematical Problems in Engineering*, vol. 2, pp. 1-6.
- Wang, C.; Shen, Y.; Zou, Y.; Li, T.; Feng, X.** (2018): Stiffness degradation characteristics destructive testing and finite-element analysis of prestressed concrete *t*-beam. *Computer Modeling in Engineering & Sciences*, vol. 114, no. 1, pp. 75-93.

Wang, Z. B.; Tao, Z.; Han, L. H.; Uy, B.; Lam, D. et al. (2017): Strength, stiffness and ductility of concrete-filled steel columns under axial compression. *Engineering Structures*, vol. 135, pp. 209-221.

Wang, Z. B.; Tao, Z.; Yu, Q. (2017): Axial compressive behaviour of concrete-filled double-tube stub columns with stiffeners. *Thin-Walled Structures*, vol. 120, no. 11, pp. 91-104.

Yang, Y. F.; Hou, C. (2017): Performance of partially compressed CFST columns through dissimilarly shaped bearing plates under axial load. *Thin-Walled Structures*, vol. 120, pp. 333-354.

Young, B.; Ellobody, E. (2006): Experimental investigation of concrete-filled cold-formed high strength stainless steel tube columns. *Journal of Constructional Steel Research*, vol. 62, no. 5, pp. 484-492.